MNRAS 000, 1–8 (2023) Preprint 16 November 2023 Compiled using MNRAS LaTeX style file v3.0

Search and characterization of third-body candidates around binary systems using Kepler and TESS data

Jefferson R. P. Inácio,[1] Isaac M. Macêdo,[1] Éder V. X. Ferreira,[2] Ronai Lisboa,[2] Tarciro N. C. Mendes,[2] Marildo G. Pereira,[3] José R. P. da Silva,[1] and Leonardo A. Almeida[1,2]★
[1]*Departamento de Física, Universidade do Estado do Rio Grande do Norte, Mossoró, RN, Brazil*
[2]*Escola de Ciências e Tecnologia, Universidade Federal do Rio Grande do Norte, Natal, RN, Brazil*
[3]*Departamento de Física, Universidade Estadual de Feira de Santana, Feira de Santana, BA, Brazil*

Accepted XXX. Received YYY; in original form ZZZ

ABSTRACT
The study of the orbital period variation of short-period binary systems has been important to understand several physical phenomena, such as the emission of gravitational waves, angular momentum loss via magnetic braking, matter transfer between the components, apsidal motion, quadrupole moment variation and presence of circumbinary bodies. With the advent of large space missions, e.g. Kepler and TESS (Transiting Exoplanet Survey Satellite), an enormous amount of high-precision photometric data with temporal coverage from years to decades has become available. Thus, in this work, we propose to study the orbital period variation of a sample of 240 binary that was observed by Kepler and TESS and, therefore, with a temporal coverage of more than 14 years. The main goal of this paper is the search and characterization of third bodies. Based on the periodicity analysis of the O-C diagram of the sample, 75 of them showed periodic variation and, therefore, were classified as binary systems with third-body candidates, while the remaining 165 did not show periodic variations. This result represents a twofold increase in tertiary candidates around binary systems compared to the study carried out with only Kepler data and is in line with what is found in the literature for stellar multiplicity.

Key words: binaries: eclipsing – binaries: close – catalogues – stars: kinematics and dynamics – methods: data analysis

1 INTRODUCTION

Binary stars, which consist of two stars orbiting a common center of mass, have contributed richly to several areas in Astrophysics (e.g., Sana et al. 2012; Grundahl et al. 2008; Clausen et al. 2008). A subclass of these systems, the eclipsing binaries, which have their orbital planes in the observer's line of sight and therefore eclipse each other, are used to determine distances and calculate fundamental parameters of stars (e.g. mass and radii) to test models of stellar evolution (e.g., Pietrzyński et al. 2012; Almeida et al. 2015, 2017).

Another topic of fundamental importance in eclipsing binary systems is the study of orbital period variation. They are used to understand various physical phenomena, e.g. emission of gravitational waves (Hulse & Taylor 1975), loss of angular momentum via magnetic braking (Tout & Hall 1991), transfer of matter between components (Tout & Hall 1991; Cehula & Pejcha 2023), apsidal motion (Gimenez & Garcia-Pelayo 1983), variation of quadrupole momentum (Applegate & Patterson 1987) and the presence of circumbinary bodies (Correia et al. 2016). In the latter scenario, the additional bodies could be planets, and therefore, crucial to understand how these objects are formed and how they evolve around two parent stars (Martin & Triaud 2015).

The characterization of binary, triple or higher order systems becomes crucial for us to understand several stellar physical processes, e.g. Tidal friction, Kozai cycles, mass transfer, angular momentum loss, merging (Tokovinin et al. 2006; Tokovinin 1997; Sana & Evans 2010; Duchêne & Kraus 2013; Sana 2016), which we would not be able to observe in isolated stars. Furthermore, we know that the way to directly measure the mass of a star is through a binary system.

Space missions, such as Kepler and TESS (*Transiting Exoplanet Survey Satellite*), have contributed significantly to the discoveries of planets around single stars and in multiple systems (e.g., Batalha et al. 2011; Borucki 2016; Astudillo-Defru et al. 2020; Gandolfi et al. 2018). Kepler, launched by NASA (North American Space Agency), began its mission in 2009 and had as its main scientific objective to detect exoplanets by the method of planetary transits, with emphasis on terrestrial planets ($R < 2.5R_{\oplus}$), located within the habitable zones of Sun-like stars (Borucki et al. 2010). To continue with the mission to discover exoplanets, the TESS space telescope was launched in 2018 by NASA, and it is still in full operation intending to search for planets that transit bright stars close to our Solar system (Ricker et al. 2014).

Combining data from the Kepler and TESS satellites, with temporal coverage of more than 14 years of observation, provides an excellent opportunity to study long-term phenomena. In this context, this paper aims to study the orbital period variation of the eclipsing binary systems observed by the Kepler and TESS satellites. To do so, we selected a sample of 240 eclipsing binary systems reported

★ E-mail: leonardo.almeida@ufrn.br

Table 1. Inner binary orbital period ($P_{\rm bin}$), orbital period (P_3) and eccentricity (e_3) of the third body derived by Conroy et al. (2014).

KIC	P_{bin} (d)	P_3 (d)	e_3
1868650	0.585		
2162283	0.906		
2450566	1.845	984 ± 473	0.31 ± 0.02
2557430	1.298		
2694741	0.327		

Notes: Table 1 is published in its entirety in the machine-readable format.

by Conroy et al. (2014) with data from both missions. The analysis of the orbital period variation of these systems will be done through the O-C (Observed minus Calculated) diagrams, see e.g. (Conroy et al. 2014; Almeida et al. 2019), and classified in cyclic and non-cyclic variations. For the systems with cyclic variations, it will be investigated if additional bodies can explain their O-C diagrams.

This paper is organized as follows. The Section 2 we present the data used for our study and data processing. In Section 3 we present the determination of the period of the binary system, the construction of the phase diagram, the determination of the eclipse times, and the adjustment for the third body in our data. Finally, in Section 4 we present the results of this study and discuss them in Section 5.

2 SAMPLE SELECTION AND DATA PROCESSING

For this study, we use a sample of 240 binary systems selected out of 1279 targets reported by Conroy et al. (2014). The selection criterion was that the binaries have been observed by the Kepler and TESS satellites. Combining both data sets, the temporal baseline of observations for all targets is more than 14 years. In Table 1, we list all targets with the inner binary's orbital period, eccentricity, and orbital period of the third body reported by Conroy et al. (2014).

trocar a ordem para ficar em acordo com a tabela

Não estão na Tabela 1

As we can see in Table 1, for some targets, e.g. KIC 3221207 and KIC 3936357, due to the relatively short temporal coverage of Kepler data, considering the long-term variations of the possible third bodies, Conroy et al. (2014) do not provide the values for their eccentricities.

To search and download the Kepler and TESS light curves from the MAST webpage[1], we used the `Lightkurve` python package (Lightkurve Collaboration et al. 2018). The presearch data conditioned simple aperture photometry (PDCSAP) flux from both Kepler and TESS satellites have been chosen for our analysis. The PDCSAP pipeline tries to remove systematic effects, e.g. long-term trends, discontinuities within the quarters, etc. For our sample, Kepler data are available in long cadence (30 minutes), while TESS data are available in long (30 minutes) and short (2 minutes) cadences. For our proposal, due to the best temporal precision, we use the TESS short cadence data.

Additional steps for the light curve preparation were done. We use the `flatten` function from `Lightkurve` to remove the low-frequency trend using the `Savitzky-Golay` filter from `Scipy` package and normalize the light curve. Besides, the `remove_outliers` function from `Lightkurve` which removes the outliers points from the light curves based on the `sigma-clipping` algorithm was used.

[1] https://archive.stsci.edu/

3 DATA ANALYSIS

The main goal of this paper is to search for variations in the O-C diagram of our selected binaries that could indicate third bodies around them. To do so, we perform the following steps: (i) determine the orbital period of the system and build its phase diagram; (ii) perform a Polyfit adjustment to obtain the eclipse instants and build the O-C diagram via a linear ephemeris; and (iii) analyze the binary orbital period variation using the O-C diagram. These steps are done in the following sections.

3.1 Period determination and phase diagram construction

As the Kepler and TESS data are not uniformly spaced in time, see Figure 1, to determine the binary orbital period, the Lomb-Scargle (LS) method (Lomb 1976; Scargle 1982) was used via `Lightkurve` program. Figure 2 shows the LS periodogram for the KIC 5513861 (TIC 120251815) system.

Having determined the period of the system, Fig. 2, we use the `stringlength` tool (Dworetsky 1983), a method of `pyTiming` from the PyAstronomy[2] library (Czesla et al. 2019), for a refinement of the obtained period. This method is suitable for non-sinusoidal periodic variations, e.g. eclipsing binaries, planetary transit, etc, returning as output the sum of the lengths among the points measured in the phase diagram, which is constructed for a period grid, see Fig. 3. The minimum output value gives the best period for the data considering the searched range.

Finally, we phase the light curve using the period of the binary system calculated in the previous step. To construct the phase diagram, we use the `fold` command of the `Lightkurve` program. The result for KIC 5513861 system is shown in Figure 4.

3.2 Determining the period variations

To determine the eclipse times of our close binary sample, we perform the same procedure done by Conroy et al. (2014). In short, the phased light curves of the binary systems are divided into four parts and each one is fitted by a chain of nth-order polynomial $P(x)$, as described in Prša et al. (2008). The fitting procedure is done using a computational algorithm called `Polyfit` which is available by Prša et al. (2008). This code is based on two principles: (i) $P(x)$ differentiable at nodes is not required, it allows breaking the polynomial chain, and (ii) the nodes can change their positions iteratively driving the solution to the nearest minimum.

In our analysis, we adopt a 2nd order polynomial with 10000 iterations and a step of 0.04 in phase for the search of each node. Thus, four polynomial solutions were derived and added to provide the general solution for the phased light curve, see one example in Fig 4. Concerning this last solution, we calculate the phase shift in each cycle of the binary, which multiplied by the orbital period gives the O-C diagram, see Fig. 7. A detailed and complete description of the algorithm is available at Prša et al. (2008).

3.3 Search for periodic signal in the O-C Diagram

With the O-C diagram of our sample in hand, the next step is to search for periodic variations that may indicate possible additional components gravitationally interacting with the binary. To do this, we apply the same procedure done in Section 3.1. To consider a reliable

[2] https://github.com/sczesla/PyAstronomy

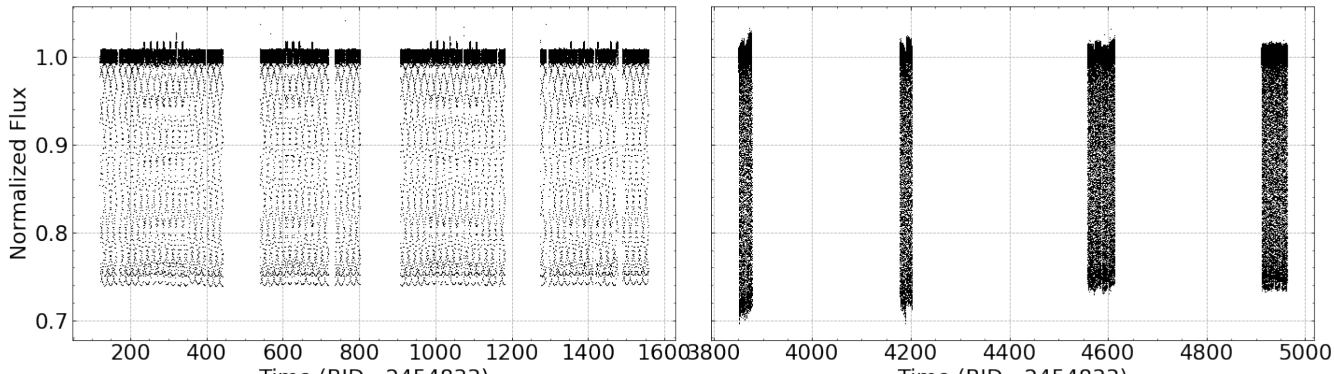

Separar melhor...

Figure 1. Normalized light curve from Kepler data (left panel) and TESS data (right panel) of KIC 5513861 (TIC 120251815).

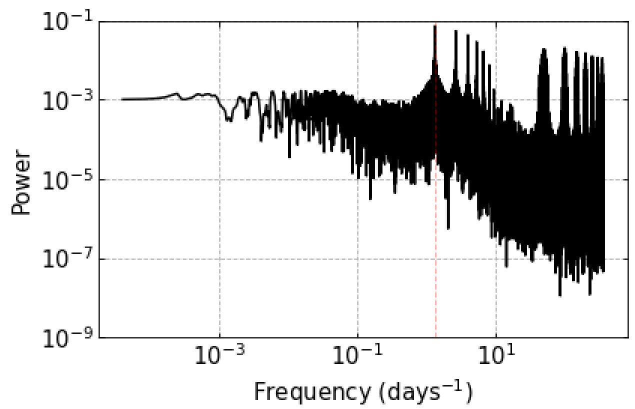

Figure 2. Lomb-Scargle periodogram obtained from the KIC 5513861 light curve. The vertical red dashed line shows the frequency with the highest power.

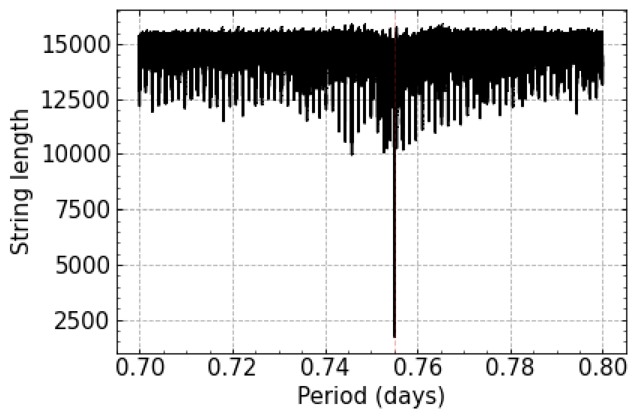

Figure 3. `Stringlength` periodogram used to refine the period determination of the KIC 5513861 object. The vertical red dashed line shows the period with the lower string length.

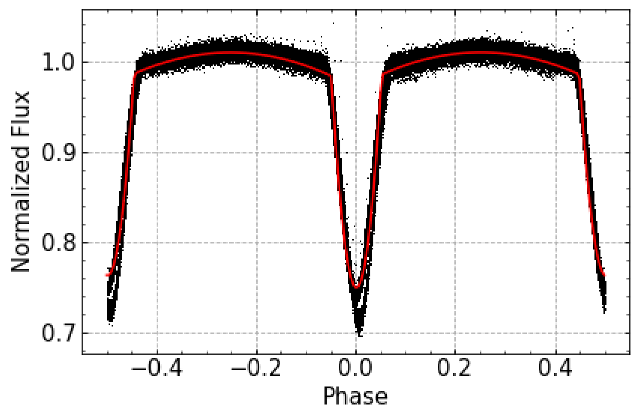

Figure 4. Phase diagram of KIC 5513861. The red line represents the best solution derived by the Polyfit program.

period, we adopted frequencies in the Lomb-Scargle periodogram above 10% of false alarm probability (FAP). As an example, Figure 5 shows the Lomb-Scargle periodogram generated from the O-C diagram data of KIC 5513861. In total, 75 of the 240 binaries analyzed show clear periodic variations in their orbital period. These systems will be analyzed in the context of light travel time in the next section.

4 RESULTS

By analyzing the Lomb-Scargle periodogram generated from the O-C diagram of 240 close binary stars, we obtained a total of 75 systems that showed clear periodic variation in their O-C diagrams (see Section 3.3). For these binaries, we analyse the period variation in the context of a third component gravitationally interacting with the inner binary, see Section 4.1.

For the remaining 165 objects, we do not identify any significant periodic variations, see one example in Figure 6. The binary orbital period, Kepler and TESS light curves, Lomb-Scargle and string-length periodograms, orbital phase diagram, and O-C diagram from these targets are available at our online tertiary candidates catalog. The analysis and discussion of the possible causes for these binaries are beyond the scope of this paper and, therefore, will be carried out in future works.

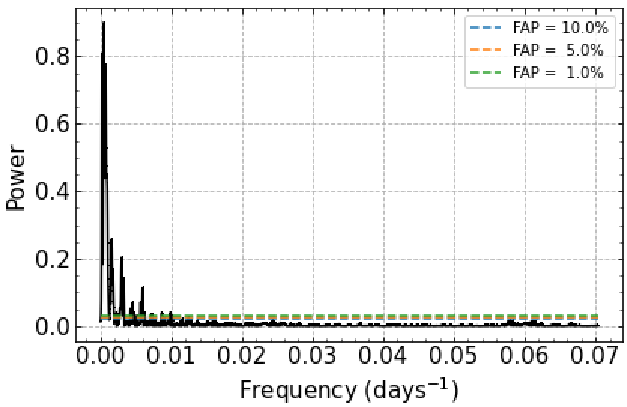

sem P maiusculo.... no restante do texto sempre "p" minusculo

Figure 5. Lomb-scargle Periodogram of the O-C diagram data of KIC 5513861. The green, orange, and blue dashed lines indicate 1%, 5%, and 10% for the false alarm probability levels, respectively.

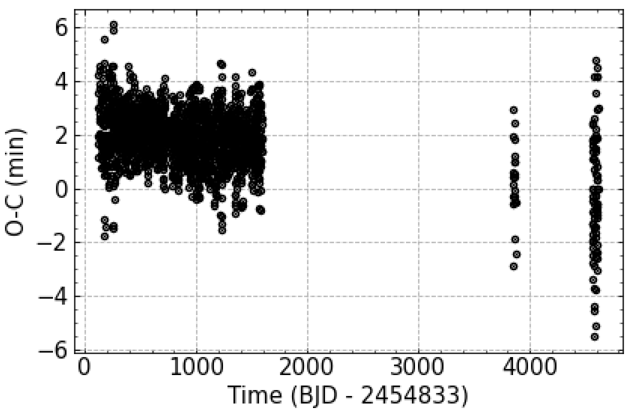

Figure 6. O-C diagram for the binary system KIC 1868650 (TIC 137306463).

4.1 Light Travel Time Effect

The Light Travel Time (LTT) effect is caused by the presence of an invisible body gravitationally interacting with an object of interest, in our case a close binary system, and consists of periodic variations in the arriving time of a periodic intrinsic signal, e.g. eclipsing times from the binary.

The variation caused by the **LTT** effect in the binary orbital period, can be mathematically described as follows (Irwin 1952):

$$\tau = \frac{a \sin i}{c} \frac{1 - e^2}{1 + e \cos f} \sin(f + \omega), \tag{1}$$

where a is the semi-major axis, e is the eccentricity, i is the orbital inclination with respect to the plane of the sky, ω is the periastron argument, f is the true anomaly, and c the speed of light.

In addition to the LTT effect, the O-C diagram of some of these systems showed long-term changes in their orbital period. Thus, for such systems, we added a linear term to Eq. 1 to fit the data and obtain the general solution, as illustrated in Fig. 8.

The fitting procedure was done in two steps. Initially, to find a preliminary solution, the `Optimize Curve Fit` task from `SciPy` library was executed. In the second step, we run a Markov Chain

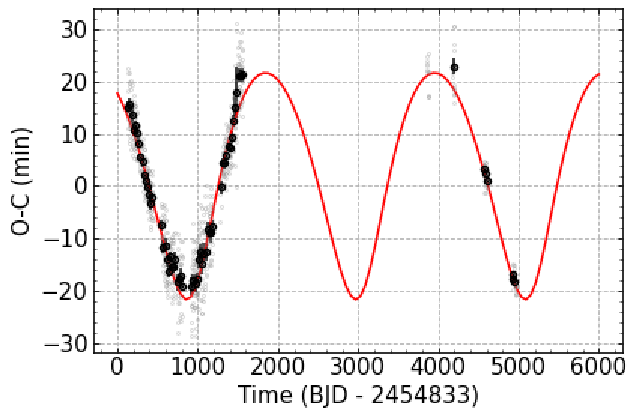

Figure 7. O-C diagram for the binary system KIC 5513861 (TIC 120251815). Individual and average of 20 measurements are shown with gray and black points, respectively. The red curve represents the best fit considering a third body around the inner binary.

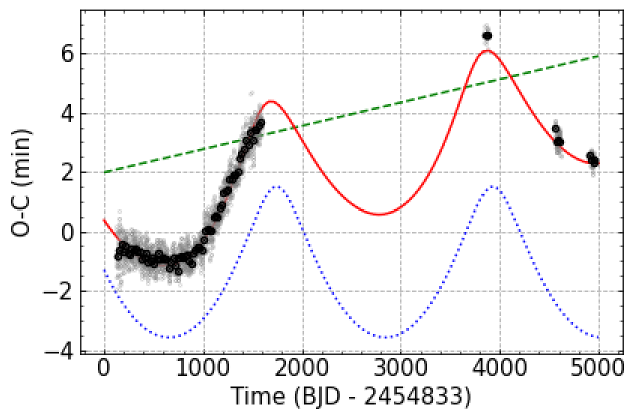

Figure 8. O-C diagram for the binary system KIC 3221207 (TIC 121213501). Individual and average of 20 measurements are shown with gray and black points. The red curve is the best solution obtained when using the sum of the LLT effect (dotted blue curve) plus the linear term (dashed green line).

Monte Carlo (MCMC) procedure through emcee program (Foreman-Mackey et al. 2013), using the preliminary solution as an initial guess, to obtain the final solution, as well as, the error bars in each fitted parameter. Figures 7 and 8 show two results of our fitting procedure, the first with only the LTT effect and the second with the addition of the linear term. An example of the results for the 75 systems with periodic variations is presented in Section A and the fitted parameters for all systems are listed in Tables 2 and C1. All results for these systems are available at our online tertiary candidates catalog

5 DISCUSSIONS

Our sample of 240 close binaries was divided into two main groups: (1) systems with periodic variations in their O-C diagrams, which were fitted with an LTT curve or an LTT curve plus a linear function, and (2) systems with non-periodic variations, which are defined as those that despite having short, increasing, decreasing or random variations in their O-C diagrams, such variations do not have an associated period with statistical significance according to the FAP.

Following the same criteria adopted by Conroy et al. (2014), we divided our sample with periodic variations into 3 subgroups according to the periods found in the O-C diagrams and the temporal baseline of the Kepler and TESS data: objects with (i) periods less than 2400 days (P < 2400 days), (ii) periods greater or equal than 2400 and less or equal than 4800 days (2400 ≤ P(days) ≤ 4800), and (iii) periods greater than 4800 days (P > 4800 days). We obtained 45, 15, and 15 systems for these three subgroups, respectively. Table 2 shows these systems according to this classification and the orbital periods and eccentricities for the third-body candidates.

In order to compare our results with those obtained by Conroy et al. (2014), in Table 3 we divided the systems with the same range of period as adopted by the last authors, i.e., P < 700 days, (700 ≤ P(days) < 1400), and P > 1400 days. In these three ranges, we and Conroy et al. (2014) found: (i) 8 and 9 systems; (ii) 10 and 9 systems, and (iii) 57 and 16 systems, respectively. This result is illustrated in Figure 9. Thus, as expected by adding TESS data and increasing the observational baseline, we found 75 close binaries with third-body candidates, ~2.1 times more systems than Conroy et al. (2014) in the sample of 240 systems. Our result represents a rate of ~31% of tertiary candidates in this sample of close binaries. It is also important to note that most of the new systems found in this study are in the range of P > 1400 days.

When considering the number of cycles for the third-body candidates observed in the data, Conroy et al. (2014) found 9 systems with at least two cycles, 9 with at least one cycle, and 16 targets with less than one cycle, while in this study we found 45, 15 and 15 systems for same ranges, respectively.

In addition to new systems with periodic variations in their orbital periods, with the combined data from Kepler and TESS and using the MCMC procedure, we were able to better estimate the parameters of the third-body candidates, such as orbital periods and eccentricities. Table 3 summarises these parameters obtained in our fit in comparison with those from Conroy et al. (2014).

Among the systems presented in Tables 2 and 3, 46 systems do not have values defined in the Conroy et al. (2014) paper for a possible third body, and 16 of them have only an approximated value for the third body period. Only four systems reported by Conroy et al. (2014) with third-body candidates were not identified by us.

The relationship between the periods of the inner binaries and the third-body candidates measured in this paper and by Conroy et al. (2014) can be visualised in Fig. 9. There is no significant difference between our measurements and those carried out by Conroy et al. (2014) for the orbital period measurements of the inner binaries. It is evident that ~97% of binaries with potential third-body candidates have periods shorter than 4 days and that there is no presence of binary systems with periods longer than 12 days (P > 12) with potential tertiary companions, consistent with results obtained by Tokovinin et al. (2006).

ACKNOWLEDGEMENTS

JRPI and IMM acknowledge the financial support from Coordenação de Aperfeiçoamento de Pessoal de Nível Superior (CAPES). LAA thanks the Conselho Nacional de Desenvolvimento Científico e Tecnológico (CNPq) for funding through process number 315502/2021.

Table 2. Binary systems with periodic variations in their O-C diagrams. The targets are divided into three intervals: periods less than 2400 days, between 2400 and 4800 days, and greater than 4800 days.

KIC	P_3 (d)	e_3	timebase (d)
2162283	2307^{+45}_{-73}	$0.64^{+0.15}_{-0.12}$	4465
2450566	1059^{+23}_{-29}	$0.655^{+0.105}_{-0.066}$	3757
2708156	$1437.2^{+13.9}_{-7.6}$	$0.087^{+0.167}_{-0.065}$	4870
3221207	2254^{+72}_{-62}	$0.426^{+0.048}_{-0.040}$	4840
3228863	$663.6^{+6.2}_{-15.3}$	$0.22^{+0.17}_{-0.15}$	4870
3936357	2133^{+68}_{-47}	$0.120^{+0.075}_{-0.061}$	4840
4451148	$769.4^{+6.8}_{-10.8}$	$0.466^{+0.087}_{-0.023}$	4840
4647652	755^{+19}_{-13}	$0.25^{+0.29}_{-0.15}$	4870
4909707	$513.87^{+0.62}_{-0.57}$	$0.664^{+0.023}_{-0.027}$	4840
4945588	1608^{+29}_{-141}	$0.871^{+0.046}_{-0.045}$	4870
4999260	2206^{+415}_{-111}	$0.790^{+0.046}_{-0.038}$	4870
5022573	1827^{+114}_{-113}	$0.766^{+0.083}_{-0.061}$	3760
5264818	$282.4^{+1.8}_{-4.2}$	$0.529^{+0.095}_{-0.045}$	4870
5513861	$2113.3^{+5.9}_{-6.3}$	$0.315^{+0.019}_{-0.029}$	4840
5975712	$1693.9^{+1.5}_{-1.4}$	$0.2180^{+0.0010}_{-0.0010}$	3780
6187893	$2028.9^{+5.8}_{-5.8}$	$0.9690^{+0.0040}_{-0.0060}$	4840
6205460	2312^{+84}_{-29}	$0.426^{+0.019}_{-0.071}$	4870
7375612	$2123.5^{+15.3}_{-7.6}$	$0.098^{+0.074}_{-0.028}$	4870
7385478	1360^{+76}_{-101}	$0.78^{+0.15}_{-0.36}$	4870
7431703	1820^{+43}_{-105}	$0.448^{+0.121}_{-0.158}$	4870
7440742	2003^{+134}_{-126}	$0.9830^{+0.0050}_{-0.0130}$	4870
7765894	$463.8^{+3.5}_{-5.4}$	$0.270^{+0.073}_{-0.088}$	4870
7766185	1886^{+43}_{-51}	$0.940^{+0.011}_{-0.013}$	4870
7816201	2328^{+210}_{-398}	$0.696^{+0.074}_{-0.124}$	4840
7938870	2102^{+31}_{-34}	$0.636^{+0.029}_{-0.019}$	4840
8043961	$422.7^{+1.6}_{-1.5}$	$0.40^{+0.19}_{-0.12}$	4870
8045121	891^{+14}_{-18}	$0.349^{+0.085}_{-0.122}$	3785
8231231	1909^{+50}_{-54}	$0.949^{+0.021}_{-0.033}$	3785
8285349	2043^{+16}_{-55}	$0.522^{+0.022}_{-0.218}$	4870
8386865	$294.3^{+1.0}_{-0.87}$	$0.421^{+0.055}_{-0.033}$	3785
8579707	1945^{+204}_{-25}	$0.523^{+0.090}_{-0.037}$	4870
9083523	2201^{+36}_{-16}	$0.370^{+0.084}_{-0.090}$	4870
9181877	1830^{+20}_{-49}	$0.596^{+0.054}_{-0.051}$	4870
9365025	$731.6^{+3.6}_{-2.2}$	$0.960^{+0.0020}_{-0.0030}$	3785
9402652	$1498.5^{+1.8}_{-1.7}$	$0.816^{+0.031}_{-0.026}$	4870
9657096	1830^{+97}_{-27}	$0.607^{+0.034}_{-0.077}$	3785
10226388	$924.4^{+9.4}_{-1.9}$	$0.518^{+0.238}_{-0.031}$	4900
10389982	2300^{+103}_{-37}	$0.839^{+0.111}_{-0.090}$	4870
10724533	1936^{+52}_{-29}	$0.426^{+0.035}_{-0.185}$	4870
10789421	456^{+10}_{-18}	$0.52^{+0.28}_{-0.18}$	4870
10818544	1872^{+164}_{-114}	$0.972^{+0.010}_{-0.021}$	3785
10979669	1532^{+55}_{-21}	$0.9740^{+0.0080}_{-0.0130}$	4870
11572643	2290^{+48}_{-47}	$0.50^{+0.31}_{-0.20}$	4900
12216817	1509^{+28}_{-41}	$0.619^{+0.071}_{-0.084}$	3785
12305537	$2044.343^{+6.0}_{-6.3}$	$0.707^{+0.037}_{-0.038}$	4900
3953981	2862^{+95}_{-123}	$0.223^{+0.095}_{-0.069}$	4870
4450976	2546^{+161}_{-204}	$0.31^{+0.15}_{-0.20}$	3760
4851217	2474^{+318}_{-147}	$0.876^{+0.083}_{-0.056}$	4870
6353203	$2449.6^{+19.4}_{-7.1}$	$0.575^{+0.057}_{-0.069}$	4870
7259917	4729^{+442}_{-197}	$0.720^{+0.063}_{-0.222}$	4840
7690843	2715^{+60}_{-72}	$0.752^{+0.058}_{-0.152}$	4870
7950962	3085^{+100}_{-117}	$0.075^{+0.053}_{-0.055}$	4870
8189196	3903^{+25}_{-31}	$0.9800^{+0.0030}_{-0.0040}$	4870
8758161	2942^{+187}_{-137}	$0.688^{+0.088}_{-0.170}$	4870

Table 2 – *continued* A table continued from the previous one.

9345838	$2497.1^{+5.2}_{-7.1}$	$0.9690^{+0.0130}_{-0.0090}$	4870
9760531	3000^{+108}_{-36}	$0.9720^{+0.0080}_{-0.0160}$	4870
10155563	3569^{+17}_{-16}	$0.9890^{+0.0010}_{-0.0020}$	4840
10259530	4584^{+136}_{-316}	$0.558^{+0.040}_{-0.044}$	4870
10481912	4102^{+96}_{-510}	$0.35^{+0.14}_{-0.12}$	4900
11255667	4715^{+412}_{-203}	$0.27^{+0.11}_{-0.14}$	4870
3448245	8314^{+298}_{-90}	$0.753^{+0.051}_{-0.014}$	4870
4909422	6583^{+927}_{-1415}	$0.839^{+0.131}_{-0.096}$	4840
5296877	4962^{+11}_{-16}	$0.7280^{+0.0100}_{-0.0070}$	4870
6462057	4926^{+360}_{-147}	$0.637^{+0.080}_{-0.177}$	4870
7457163	6256^{+135}_{-194}	$0.527^{+0.062}_{-0.039}$	4870
7512381	6805^{+249}_{-135}	$0.411^{+0.040}_{-0.131}$	4870
8397460	8113^{+510}_{-443}	$0.9660^{+0.0030}_{-0.0030}$	4870
8587792	5493^{+294}_{-278}	$0.380^{+0.046}_{-0.040}$	4870
8894630	7636^{+351}_{-316}	$0.737^{+0.043}_{-0.030}$	4870
9602595	6557^{+176}_{-624}	$0.762^{+0.037}_{-0.028}$	4870
9612468	7444^{+488}_{-417}	$0.620^{+0.044}_{-0.051}$	3785
9832227	6091^{+143}_{-115}	$0.507^{+0.028}_{-0.047}$	4870
10485137	5844^{+412}_{-145}	$0.639^{+0.072}_{-0.064}$	4900
10711938	6689^{+261}_{-316}	$0.631^{0.250}_{-0.059}$	4080
12157987	2662^{+58}_{-38}	$0.914^{+0.034}_{-0.057}$	4900

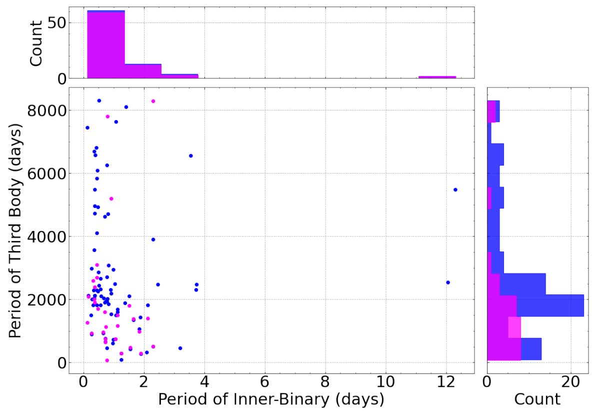

Figure 9. Period of the third-body candidates versus period of the inner binary. The blue and magenta points represent our measurement and the results from Conroy et al. (2014), respectively. The top and right histograms represent the count of binaries and third-body candidates in function of their orbital periods, respectively.

DATA AVAILABILITY

The online tertiary candidates catalog provides the results for all close binaries, with and without periodic orbital period variations, studied in this paper.

The Kepler and TESS data are available via the python-based package LightKurve.

REFERENCES

Almeida L., et al., 2015, The Astrophysical Journal, 812, 102
Almeida L., et al., 2017, Astronomy & Astrophysics, 598, A84
Almeida L. A., et al., 2019, AJ, 157, 150
Applegate J. H., Patterson J., 1987, The Astrophysical Journal, 322, L99
Astudillo-Defru N., et al., 2020, Astronomy & Astrophysics
Batalha N. M., et al., 2011, The Astrophysical Journal, 729
Borucki W. J., 2016, Reports on Progress in Physics, 79
Borucki W. J., et al., 2010, Science, 327, 977
Cehula J., Pejcha O., 2023, MNRAS, 524, 471
Clausen J., Torres G., Bruntt H., Andersen J., Nordström B., Stefanik R., Latham D. W., Southworth J., 2008, Astronomy & Astrophysics, 487, 1095
Conroy K. E., Prša A., Stassun K. G., Orosz J. A., Fabrycky D. C., Welsh W. F., 2014, The Astronomical Journal, 147, 45
Correia A. C., Boué G., Laskar J., 2016, Celestial Mechanics and Dynamical Astronomy, 126, 189
Czesla S., Schröter S., Schneider C. P., Huber K. F., Pfeifer F., Andreasen D. T., Zechmeister M., 2019, PyA: Python astronomy-related packages (ascl:1906.010)
Duchêne G., Kraus A., 2013, ARA&A, 51, 269
Dworetsky M., 1983, Monthly Notices of the Royal Astronomical Society, 203, 917
Foreman-Mackey D., Hogg D. W., Lang D., Goodman J., 2013, Publications of the Astronomical Society of the Pacific, 125, 306
Gandolfi D., et al., 2018, Astronomy & Astrophysics
Gimenez A., Garcia-Pelayo J. M., 1983, Astrophysics and Space Science, 92, 203
Grundahl F., Clausen J., Hardis S., Frandsen S., 2008, Astronomy & Astrophysics, 492, 171
Hulse R. A., Taylor J. H., 1975, The Astrophysical Journal, 195, L51
Irwin J. B., 1952, The Astrophysical Journal, 116, 211
Lightkurve Collaboration et al., 2018, Lightkurve: Kepler and TESS time series analysis in Python, Astrophysics Source Code Library (ascl:1812.013)
Lomb N. R., 1976, Astrophysics and space science, 39, 447
Martin D. V., Triaud A. H., 2015, Monthly Notices of the Royal Astronomical Society: Letters, 455, L46
Pietrzyński G., et al., 2012, Proceedings of the International Astronomical Union, 8, 169
Prša A., Guinan E., Devinney E., DeGeorge M., Bradstreet D., Giammarco J., Alcock C., Engle S., 2008, The Astrophysical Journal, 687, 542
Ricker G. R., et al., 2014, Journal of Astronomical Telescopes, Instruments, and Systems, 1, 014003
Sana H., 2016, Proceedings of the International Astronomical Union, 12, 110
Sana H., Evans C. J., 2010, Proceedings of the International Astronomical Union, 6, 474
Sana H., et al., 2012, Science, 337, 444
Scargle J. D., 1982, The Astrophysical Journal, 263, 835
Tokovinin A., 1997, Astronomy Letters, 23, 727
Tokovinin A., Thomas S., Sterzik M., Udry S., 2006, Astronomy & Astrophysics, 450, 681
Tout C. A., Hall D. S., 1991, Monthly Notices of the Royal Astronomical Society, 253, 9

APPENDIX A: BINARY SYSTEMS WITH PERIODIC ORBITAL PERIOD VARIATIONS

As mentioned in Section 3.3, of the 240 binary systems in our sample, 75 systems, ∼31% of the sample, show periodic variations in their O-C diagrams. In this section, we present a target as an example of the analysis and results of these systems and the parameters obtained for the possible third body. All results from these 75 systems can be accessed online in the tertiary candidates catalog.

KIC 2450566 is one of the systems that present periodic variation in its O-C diagram, see Fig. A1, indicating the presence of a third body around the inner binary. The best fit for the tertiary candidate yields: orbital period $P = 1059^{+23}_{-29}$ d; eccentricity $e = 0.655^{+0.105}_{-0.066}$; projected semi-major axis of $a \sin i = 1.0326^{+0.13}_{-0.10}$ au; and perias-

Table 3. Comparison between results of period and eccentricity for the third-body candidates found in this paper (P_3 and e_3) and in Conroy et al. (2014) ($P_{3,C}$ and $e_{3,C}$).

KIC	P_3 (d)	$P_{3,C}$ (d)	e_3	$e_{3,C}$	timebase (d)
3228863	$663.6^{+6.2}_{-15.3}$	644 ± 16	$0.22^{+0.17}_{-0.15}$	0.0000 ± 0.0030	4870
3641446		228.6 ± 1.0		0.000 ± 0.010	3760
4909707	$513.87^{+0.62}_{-0.57}$	516 ± 16	$0.664^{+0.023}_{-0.027}$	0.000 ± 0.010	4840
5264818	$282.4^{+1.8}_{-4.2}$	300 ± 108	$0.529^{+0.095}_{-0.045}$	0.42 ± 0.31	4870
7690843*	2715^{+60}_{-72}	74.1 ± 0.1	$0.752^{+0.058}_{-0.152}$	0.233 ± 0.021	4870
7765894	$463.8^{+3.5}_{-5.4}$		$0.270^{+0.073}_{-0.088}$		4870
8043961	$422.7^{+1.6}_{-1.5}$	478 ± 10	$0.40^{+0.19}_{-0.12}$	0.000 ± 0.005	4870
8386865	$294.3^{+1.0}_{-0.87}$	294 ± 3	$0.421^{+0.055}_{-0.033}$	0.50 ± 0.01	3785
9451096		106.8 ± 0.1		0.091 ± 0.033	4870
10789421	456^{+10}_{-18}		$0.52^{+0.28}_{-0.18}$		4870
10991989		554.8 ± 64.1		0.000 ± 0.018	4900
2450566	1059^{+23}_{-29}	984 ± 473	$0.655^{+0.105}_{-0.066}$	0.31 ± 0.02	3757
4451148	$769.4^{+6.8}_{-10.8}$	746 ± 52	$0.466^{+0.087}_{-0.023}$	0.300 ± 0.004	4840
4647652	755^{+19}_{-13}	755 ± 44	$0.25^{+0.29}_{-0.15}$	0.244 ± 0.003	4870
5975712*	$1693.9^{+1.5}_{-1.4}$	1165 ± 964	$0.2180^{+0.0010}_{-0.0010}$	0.000 ± 0.013	3780
7385478	1360^{+76}_{-101}	1389 ± 795	$0.78^{+0.15}_{-0.36}$	0.245 ± 0.007	4870
8045121	891^{+14}_{-18}	939 ± 26	$0.349^{+0.085}_{-0.122}$	0.000 ± 0.001	3785
9365025	$731.6^{+3.6}_{-2.2}$		$0.960^{+0.0020}_{-0.0030}$		3785
9612468*	7444^{+488}_{-417}	1264 ± 233	$0.620^{+0.044}_{-0.051}$	0.340 ± 0.001	3785
10226388	$924.4^{+9.4}_{-1.9}$	965 ± 184	$0.518^{+0.238}_{-0.031}$	0.04 ± 0.01	4900
10724533*	1936^{+52}_{-29}	1131 ± 198	$0.426^{+0.035}_{-0.185}$	0.265 ± 0.003	4870
2162283	2307^{+45}_{-73}		$0.64^{+0.15}_{-0.12}$		4465
2708156	$1437.2^{+13.9}_{-7.6}$		$0.087^{+0.167}_{-0.065}$		4870
3221207	2254^{+72}_{-62}	~ 1700	$0.426^{+0.048}_{-0.040}$		4840
3448245	8314^{+298}_{-90}		$0.753^{+0.051}_{-0.014}$		4870
3936357	2133^{+68}_{-47}	~ 2400	$0.120^{+0.075}_{-0.061}$		4840
3953981	2862^{+95}_{-123}		$0.223^{+0.095}_{-0.069}$		4870
4450976	2546^{+161}_{-204}		$0.31^{+0.15}_{-0.20}$		3760
4758368		~ 1500			4870
4851217	2474^{+318}_{-147}		$0.876^{+0.083}_{-0.056}$		4870
4909422	6583^{+927}_{-1415}		$0.839^{+0.131}_{-0.096}$		4840
4945588	1608^{+29}_{-141}	~ 1500	$0.871^{+0.046}_{-0.045}$		4870
4999260	2206^{+415}_{-111}		$0.790^{+0.046}_{-0.038}$		4870
5022573	1827^{+114}_{-113}		$0.766^{+0.083}_{-0.061}$		3760
5296877	4962^{+11}_{-16}	~ 1900	$0.7280^{+0.0100}_{-0.0070}$		4870
5513861	$2113.3^{+5.9}_{-6.3}$	~ 1800	$0.315^{+0.019}_{-0.029}$		4840
6187893	$2028.9^{+5.8}_{-5.8}$	~ 7800	$0.9690^{+0.0040}_{-0.0060}$		4840
6205460	2312^{+84}_{-29}		$0.426^{+0.019}_{-0.071}$		4870
6353203	$2449.6^{+19.4}_{-7.1}$		$0.575^{+0.057}_{-0.069}$		4870
6462057	4926^{+360}_{-147}		$0.637^{+0.080}_{-0.177}$		4870
7259917	4729^{+442}_{-197}		$0.720^{+0.063}_{-0.222}$		4840
7375612	$2123.5^{+15.3}_{-7.6}$	~ 2100	$0.098^{+0.074}_{-0.028}$		4870
7431703	1820^{+43}_{-105}		$0.448^{+0.121}_{-0.158}$		4870
7440742	2003^{+134}_{-126}		$0.9830^{+0.0050}_{-0.0130}$		4870
7457163	6256^{+135}_{-194}		$0.527^{+0.062}_{-0.039}$		4870
7512381	6805^{+249}_{-135}		$0.411^{+0.040}_{-0.131}$		4870
7766185	1886^{+43}_{-51}		$0.940^{+0.011}_{-0.013}$		4870
7816201	2328^{+210}_{-398}		$0.696^{+0.074}_{-0.124}$		4840
7938870	2102^{+31}_{-34}		$0.636^{+0.029}_{-0.019}$		4840
7950962	3085^{+100}_{-117}		$0.075^{+0.053}_{-0.055}$		4870
8189196	3903^{+25}_{-31}	~ 8300	$0.9800^{+0.0030}_{-0.0040}$		4870
8231231	1909^{+50}_{-54}	~ 1600	$0.949^{+0.021}_{-0.033}$		3785
8285349	2043^{+16}_{-55}		$0.522^{+0.022}_{-0.218}$		4870
8397460	8113^{+510}_{-443}		$0.9660^{+0.0030}_{-0.0030}$		4870
8579707	1945^{+204}_{-25}		$0.523^{+0.090}_{-0.037}$		4870
8587792	5493^{+294}_{-278}		$0.380^{+0.046}_{-0.040}$		4870
8758161	2942^{+187}_{-137}		$0.688^{+0.088}_{-0.170}$		4870

Table 3 – *continued* A table continued from the previous one.

KIC	P_3 (d)	$P_{3,C}$ (d)	e_3	$e_{3,C}$	timebase (d)
8894630	7636^{+351}_{-316}		$0.737^{+0.043}_{-0.030}$		4870
9083523	2201^{+36}_{-16}	~ 5200	$0.370^{+0.087}_{-0.090}$		4870
9181877	1830^{+20}_{-49}	~ 2600	$0.596^{+0.054}_{-0.051}$		4870
9345838	$2497.1^{+5.2}_{-7.1}$		$0.9690^{+0.0130}_{-0.0090}$		4870
9402652	$1498.5^{+1.8}_{-1.7}$		$0.816^{+0.031}_{-0.026}$		4870
9602595	6557^{+176}_{-624}		$0.762^{+0.037}_{-0.028}$		4870
9657096	1830^{+97}_{-27}	~ 1400	$0.607^{+0.034}_{-0.077}$		3785
9760531	3000^{+108}_{-36}		$0.9720^{+0.0080}_{-0.0160}$		4870
9832227	6091^{+143}_{-115}		$0.507^{+0.028}_{-0.047}$		4870
10155563	3569^{+17}_{-16}		$0.9890^{+0.0010}_{-0.0020}$		4840
10259530	4584^{+136}_{-316}		$0.558^{+0.040}_{-0.044}$		4870
10389982	2300^{+103}_{-37}		$0.839^{+0.111}_{-0.090}$		4870
10481912	4102^{+96}_{-510}	~ 2700	$0.35^{+0.14}_{-0.12}$		4900
10485137	5844^{+412}_{-145}	~ 3100	$0.639^{+0.072}_{-0.064}$		4900
10711938	6689^{+261}_{-316}	~ 2000	$0.631^{0.250}_{-0.059}$		4080
10818544	1872^{+164}_{-114}		$0.972^{+0.010}_{-0.021}$		3785
10979669	1532^{+55}_{-21}		$0.9740^{+0.0080}_{-0.0130}$		4870
11255667	4715^{+412}_{-203}		$0.27^{+0.11}_{-0.14}$		4870
11572643	2290^{+48}_{-47}		$0.50^{+0.31}_{-0.20}$		4900
12157987	2662^{+58}_{-38}		$0.914^{+0.034}_{-0.057}$		4900
12216817	1509^{+28}_{-41}		$0.619^{+0.071}_{-0.084}$		3785
12305537	$2044.343^{+6.0}_{-6.3}$		$0.707^{+0.037}_{-0.038}$		4900

Notes: *Objects with periods identified in this document that are outside the period range indicated by Conroy et al. (2014).

tron argument $\omega = 307^{+10}_{-18}$ degrees. The 76 systems with all the parameters for their third-body candidates are listed in Table C1.

APPENDIX B: BINARY SYSTEMS WITH NON-PERIODIC ORBITAL PERIOD VARIATIONS

Based on the Lomb-Scargle periodogram of the O-C diagram data, 165 objects ($\sim$ 69%) from the sample do not show any significant periodic variations, see Section 3.3. The absence of significant variations suggests that their orbital periods are relatively stable over time. However, it is important to note that this does not necessarily mean that these systems are completely stable and will not show any long-term changes in their periods. Further observations and analyses may be necessary to confirm the stability of the orbital period of these systems over longer timescales.

Here, as a representative example of these 165 objects, we present the results of KIC 1868650, see Fig. B1. In this figure shows the Kepler and TESS light curves, the Lomb-Scargle and string-length periodograms, the phase diagram, and the derived O-C diagram. The results for all 165 binary systems can be accessed in our online tertiary candidates catalog.

APPENDIX C: TABLE WITH DERIVED PARAMETERS FOR THE THIRD-BODY CANDIDATES AND THEIR INNER BINARIES

This paper has been typeset from a TEX/LATEX file prepared by the author.

????

Table C1. Parameters derived for the inner binaries and the third-body candidates.

KIC	P_3 (d)	T_3 (BJD-2454833)	e_3	$a\sin i$ (au)	ω (°)	A (min)	B (min/d)
2162283	2307^{+45}_{-73}	1940^{+203}_{-268}	$0.64^{+0.15}_{-0.12}$	$0.92^{+0.26}_{-0.17}$	306.948^{+27}_{-44}		
2450566	1059^{+23}_{-29}	1173^{+15}_{-36}	$0.655^{+0.105}_{-0.066}$	$1.03^{+0.13}_{-0.10}$	$307.417^{+10.050}_{-17.567}$		
2708156	$1437.2^{+13.9}_{-7.6}$	$103.0^{+5.0}_{-3.6}$	$0.087^{+0.167}_{-0.065}$	$2.777^{+0.078}_{-0.136}$	$186.6^{+7.7}_{-4.4}$	$-17.9^{+1.9}_{-1.8}$	$0.00690^{+0.00040}_{-0.00030}$
3221207	2254^{+72}_{-62}	1605^{+165}_{-198}	$0.426^{+0.048}_{-0.040}$	$0.287^{+0.012}_{-0.018}$	69^{+25}_{-29}	$0.711^{+0.029}_{-0.125}$	$0.00080^{+0.00010}_{-0.00010}$
3228863	$663.6^{+6.2}_{-15.3}$	248^{+44}_{-31}	$0.22^{+0.17}_{-0.15}$	$0.458^{+0.019}_{-0.039}$	$260.6^{+23.3}_{-4.1}$		
3448245	8314^{+298}_{-90}	701^{+31}_{-12}	$0.753^{+0.051}_{-0.014}$	$0.2070^{+0.0049}_{-0.0037}$	$0.86^{+2.64}_{-0.68}$		
3936357	2133^{+68}_{-47}	4071^{+106}_{-267}	$0.120^{+0.075}_{-0.061}$	$0.326^{+0.013}_{-0.017}$	203^{+26}_{-51}	$-3.31^{+0.40}_{-0.23}$	$0.00140^{+0.00010}_{-0.00010}$
3953981	2862^{+95}_{-123}	4078^{+237}_{-314}	$0.223^{+0.095}_{-0.069}$	$0.1532^{+0.0137}_{-0.0097}$	255^{+28}_{-42}	$-0.300^{+0.045}_{-0.043}$	$0.00100^{+0.00010}_{-0.00010}$
4450976	2546^{+161}_{-204}	1612^{+350}_{-236}	$0.31^{+0.15}_{-0.20}$	$23.9^{+1.7}_{-1.9}$	297^{+35}_{-34}		
4451148	$769.4^{+6.8}_{-10.8}$	$4.1^{+0.39}_{-0.93}$	$0.466^{+0.087}_{-0.023}$	$0.63^{+0.22}_{-0.13}$	$165.1^{+1.2}_{-7.6}$		
4647652	755^{+19}_{-13}	732^{+65}_{-69}	$0.25^{+0.29}_{-0.15}$	$0.442^{+0.102}_{-0.099}$	239^{+59}_{-21}		
4851217	2474^{+318}_{-147}	205^{+14}_{-17}	$0.876^{+0.083}_{-0.056}$	$0.574^{+0.069}_{-0.069}$	102^{+13}_{-12}	$8.24^{+0.68}_{-0.53}$	$-0.00660^{+0.00050}_{-0.00040}$
4909422	6583^{+927}_{-1415}	3942^{+148}_{-353}	$0.839^{+0.131}_{-0.096}$	$0.547^{+0.027}_{-0.069}$	$6.7^{+6.8}_{-4.8}$	$6.08^{+0.73}_{-1.33}$	$-0.0024^{+0.0003}_{-0.0002}$
4909707	$513.87^{+0.62}_{-0.57}$	$1047.2^{+1.3}_{-2.4}$	$0.664^{+0.023}_{-0.027}$	$1.446^{+0.041}_{-0.049}$	$358.85^{+0.77}_{-1.35}$	$-6.82^{+0.12}_{-0.12}$	$0.002860^{+0.000050}_{-0.000060}$
4945588	1608^{+29}_{-141}	1785^{+15}_{-29}	$0.871^{+0.046}_{-0.045}$	$0.896^{+0.022}_{-0.046}$	$135^{+5.4}_{-6.4}$	$9.24^{+0.29}_{-0.65}$	$-0.00220^{+0.00030}_{-0.00010}$
4999260	2206^{+415}_{-111}	1703^{+119}_{-75}	$0.790^{+0.046}_{-0.038}$	$0.300^{+0.082}_{-0.056}$	$346.0^{+9.0}_{-14.5}$	$4.68^{+0.49}_{-0.26}$	$-0.00185^{+0.00013}_{-0.00017}$
5022573	1827^{+114}_{-113}	1896^{+104}_{-146}	$0.766^{+0.083}_{-0.061}$	$2.01^{+0.19}_{-0.21}$	26^{+13}_{-10}	$2.90^{+0.12}_{-0.14}$	$-0.00140^{+0.00010}_{-0.00010}$
5264818	$282.4^{+1.8}_{-4.2}$	403^{+10}_{-14}	$0.529^{+0.095}_{-0.045}$	$0.358^{+0.019}_{-0.033}$	$352.1^{+6.2}_{-9.9}$	$3.83^{+0.21}_{-0.27}$	$-0.000130^{+0.000020}_{-0.000040}$
5296877	4962^{+11}_{-16}	$4964.5^{+10.2}_{-9.0}$	$0.7280^{+0.0100}_{-0.0070}$	$0.6453^{+0.0035}_{-0.0044}$	$87.02^{+0.66}_{-0.69}$		
5513861	$2113.3^{+5.9}_{-6.3}$	943^{+30}_{-34}	$0.315^{+0.019}_{-0.029}$	$2.613^{+0.063}_{-0.062}$	$291.3^{+5.3}_{-5.70}$		
5975712	$1693.9^{+1.5}_{-1.4}$	$2267.6^{+2.9}_{-2.6}$	$0.2180^{+0.0010}_{-0.0010}$	$1.19315^{+0.00098}_{-0.00118}$	$262.48^{+0.31}_{-0.41}$	$25.817^{+0.029}_{-0.049}$	$-0.012010^{+0.000020}_{-0.000010}$
6187893	$2028.9^{+5.8}_{-5.8}$	1658^{+19}_{-21}	$0.9690^{+0.0040}_{-0.0060}$	$10.81^{+0.78}_{-0.81}$	$354.40^{+0.65}_{-0.70}$		
6205460	2312^{+84}_{-29}	$1052.6^{+32.8}_{-7.0}$	$0.426^{+0.019}_{-0.071}$	$26.08^{+0.15}_{-0.68}$	$233^{+4.34}_{-1.7}$		
6353203	$2449.6^{+19.4}_{-7.1}$	199^{+23}_{-18}	$0.575^{+0.057}_{-0.069}$	$1.761^{+0.097}_{-0.184}$	$33.8^{+9.9}_{-2.3}$		
6462057	4926^{+360}_{-147}	4986^{+306}_{-140}	$0.637^{+0.080}_{-0.177}$	$0.285^{+0.022}_{-0.030}$	76^{+18}_{-11}	$1.69^{+0.11}_{-0.21}$	$-0.00140^{+0.00010}_{-0.00010}$
7259917	4729^{+442}_{-197}	$61.8^{+8.1}_{-20.3}$	$0.720^{+0.063}_{-0.222}$	$0.552^{+0.087}_{-0.119}$	223^{+22}_{-17}	$5.81^{+0.84}_{-0.72}$	$0.00090^{+0.00020}_{-0.00040}$
7375612	$2123.5^{+15.3}_{-7.6}$	2360^{+235}_{-122}	$0.098^{+0.074}_{-0.028}$	$0.848^{+0.031}_{-0.013}$	303^{+39}_{-19}		
7385478	1360^{+76}_{-101}	329^{+27}_{-26}	$0.78^{+0.15}_{-0.36}$	$2.01^{+0.20}_{-0.44}$	60^{+24}_{-26}	$8.1^{+1.2}_{-2.3}$	$-0.00160^{+0.00040}_{-0.000050}$
7431703	1820^{+43}_{-105}	912^{+335}_{-216}	$0.448^{+0.121}_{-0.158}$	$0.135^{+0.031}_{-0.016}$	133^{+47}_{-38}		
7440742	2003^{+134}_{-126}	1998^{+79}_{-146}	$0.9830^{+0.0050}_{-0.0130}$	$2.205^{+0.090}_{-0.188}$	$11.4^{+1.8}_{-3.9}$	$3.96^{+0.52}_{-0.42}$	$0.00660^{+0.00040}_{-0.00030}$
7457163	6256^{+135}_{-194}	5732^{+176}_{-98}	$0.527^{+0.062}_{-0.039}$	$1.911^{+0.043}_{-0.029}$	$278.1^{+8.3}_{-3.8}$		
7512381	6805^{+249}_{-135}	801^{+71}_{-56}	$0.411^{+0.040}_{-0.131}$	$0.902^{+0.089}_{-0.029}$	$340.9^{+7.4}_{-5.2}$		
7690843	2715^{+60}_{-72}	1818^{+90}_{-86}	$0.752^{+0.058}_{-0.152}$	$1.69^{+0.27}_{-0.34}$	$340.3^{+7.8}_{-11.0}$	$-0.75^{+0.13}_{-0.16}$	$-0.00030^{+0.00010}_{-0.00010}$
7765894	$463.8^{+3.5}_{-5.4}$	101^{+50}_{-29}	$0.270^{+0.073}_{-0.088}$	$2.66^{+0.61}_{-0.28}$	143^{+34}_{-17}		
7766185	1886^{+43}_{-51}	1590^{+36}_{-13}	$0.940^{+0.011}_{-0.013}$	$0.0631^{+0.0020}_{-0.0027}$	$358.0^{+1.5}_{-2.5}$	$1.475^{+0.013}_{-0.016}$	$-0.000550^{+0.000010}_{-0.000010}$
7816201	2328^{+210}_{-398}	2395^{+84}_{-345}	$0.696^{+0.074}_{-0.124}$	$0.222^{+0.012}_{-0.016}$	61^{+36}_{-27}	$4.54^{+0.22}_{-0.50}$	$-0.00090^{+0.00010}_{-0.00010}$
7938870	2102^{+31}_{-34}	1797^{+66}_{-54}	$0.636^{+0.029}_{-0.019}$	$0.345^{+0.015}_{-0.014}$	$300.1^{+11.0}_{-6.8}$	$-7.80^{+0.18}_{-0.21}$	$0.00211^{+0.00006}_{-0.00006}$
7950962	3085^{+100}_{-117}	334^{+56}_{-36}	$0.075^{+0.053}_{-0.055}$	$0.215^{+0.013}_{-0.021}$	$172.3^{+3.8}_{-5.8}$	$1.99^{+0.13}_{-0.18}$	$0.00170^{+0.00010}_{-0.00010}$
8043961	$422.7^{+1.6}_{-1.5}$	557^{+26}_{-32}	$0.40^{+0.19}_{-0.12}$	$0.407^{+0.052}_{-0.041}$	232^{+21}_{-27}		
8045121	891^{+14}_{-18}	455^{+66}_{-82}	$0.349^{+0.085}_{-0.122}$	$0.595^{+0.091}_{-0.060}$	178^{+32}_{-32}	$0.755^{+0.138}_{-0.066}$	$0.00310^{+0.00090}_{-0.00060}$
8189196	3903^{+25}_{-31}	3871^{+16}_{-17}	$0.9800^{+0.0030}_{-0.0040}$	$8.74^{+0.65}_{-0.58}$	$352.08^{+0.67}_{-0.86}$		
8231231	1909^{+50}_{-54}	1917^{+75}_{-100}	$0.949^{+0.021}_{-0.033}$	$2.035^{+0.077}_{-0.279}$	$17.5^{+4.3}_{-4.3}$	$3.19^{+0.75}_{-0.63}$	$0.00860^{+0.00050}_{-0.00050}$
8285349	2043^{+16}_{-55}	$2184.4^{+5.6}_{-22.0}$	$0.522^{+0.022}_{-0.218}$	$1.079^{+0.026}_{-0.071}$	$0.25^{+0.66}_{-0.20}$		
8386865	$294.3^{+1.0}_{-0.87}$	$199.9^{+5.0}_{-5.5}$	$0.421^{+0.055}_{-0.033}$	$0.377^{+0.012}_{-0.013}$	$141.1^{+7.0}_{-6.1}$		
8397460	8113^{+510}_{-443}	3509^{+239}_{-442}	$0.9660^{+0.0030}_{-0.0030}$	$12.40^{+0.89}_{-0.76}$	$184.6^{+3.2}_{-3.5}$	$-2.97^{+0.81}_{-0.63}$	$0.00270^{+0.00010}_{-0.00020}$
8579707	1945^{+204}_{-25}	1775^{+45}_{-63}	$0.523^{+0.090}_{-0.037}$	$0.533^{+0.042}_{-0.016}$	274^{+12}_{-27}		
8587792	5493^{+294}_{-278}	439^{+71}_{-46}	$0.380^{+0.046}_{-0.040}$	$0.838^{+0.052}_{-0.050}$	$320.4^{+8.3}_{-6.8}$	$0.20^{+0.20}_{-0.16}$	$0.00040^{+0.00010}_{-0.00010}$
8758161	2942^{+187}_{-137}	2078^{+245}_{-277}	$0.688^{+0.088}_{-0.170}$	$3.90^{+0.89}_{-0.79}$	165^{+15}_{-23}		
8894630	7636^{+351}_{-316}	$56.9^{+24.1}_{-8.5}$	$0.737^{+0.043}_{-0.030}$	$3.85^{+0.35}_{-0.21}$	$14.4^{+4.4}_{-4.5}$		
9083523	2201^{+36}_{-16}	1109^{+49}_{-45}	$0.370^{+0.084}_{-0.090}$	$0.432^{+0.020}_{-0.021}$	$202.9^{+10.5}_{-7.4}$		
9181877	1830^{+20}_{-49}	1884^{+58}_{-122}	$0.596^{+0.054}_{-0.051}$	$1.78^{+0.20}_{-0.10}$	$44.9^{+9.2}_{-9.8}$	$4.70^{+0.30}_{-0.49}$	$-0.00070^{+0.00010}_{-0.00010}$
9345838	$2497.1^{+5.2}_{-7.1}$	$22.9^{+19.7}_{-6.8}$	$0.9690^{+0.0130}_{-0.0090}$	$2.34^{+0.65}_{-0.52}$	$6.99^{+0.82}_{-1.24}$		
9365025	$731.6^{+3.6}_{-2.2}$	$859.4^{+3.8}_{-1.4}$	$0.960^{+0.0020}_{-0.0030}$	$2.546^{+0.026}_{-0.012}$	$4.14^{+0.55}_{-0.35}$		
9402652	$1498.5^{+1.8}_{-1.7}$	$1504.1^{+4.1}_{-3.9}$	$0.816^{+0.031}_{-0.026}$	$1.029^{+0.024}_{-0.026}$	$263.6^{+1.6}_{-1.6}$	$-12.46^{+0.27}_{-0.18}$	$0.002550^{+0.000030}_{-0.000030}$
9602595	6557^{+176}_{-624}	4470^{+65}_{-110}	$0.762^{+0.037}_{-0.028}$	$25.7^{+1.2}_{-1.2}$	$191.3^{+7.9}_{-4.9}$		
9612468	7444^{+488}_{-417}	1514^{+49}_{-68}	$0.620^{+0.044}_{-0.051}$	$0.781^{+0.032}_{-0.029}$	$138.7^{+6.6}_{-7.1}$		
9657096	1830^{+97}_{-27}	3919^{+190}_{-72}	$0.607^{+0.034}_{-0.077}$	$1.340^{+0.033}_{-0.032}$	$132.9^{+8.4}_{-4.7}$	$6.87^{+0.17}_{-0.25}$	$-0.00090^{+0.00010}_{-0.00020}$
9760531	3000^{+108}_{-36}	3010^{+50}_{-119}	$0.9720^{+0.0080}_{-0.0160}$	$0.634^{+0.022}_{-0.056}$	$13.1^{+1.4}_{-1.4}$	$3.13^{+0.12}_{-0.10}$	$-0.000590^{+0.000010}_{-0.000010}$

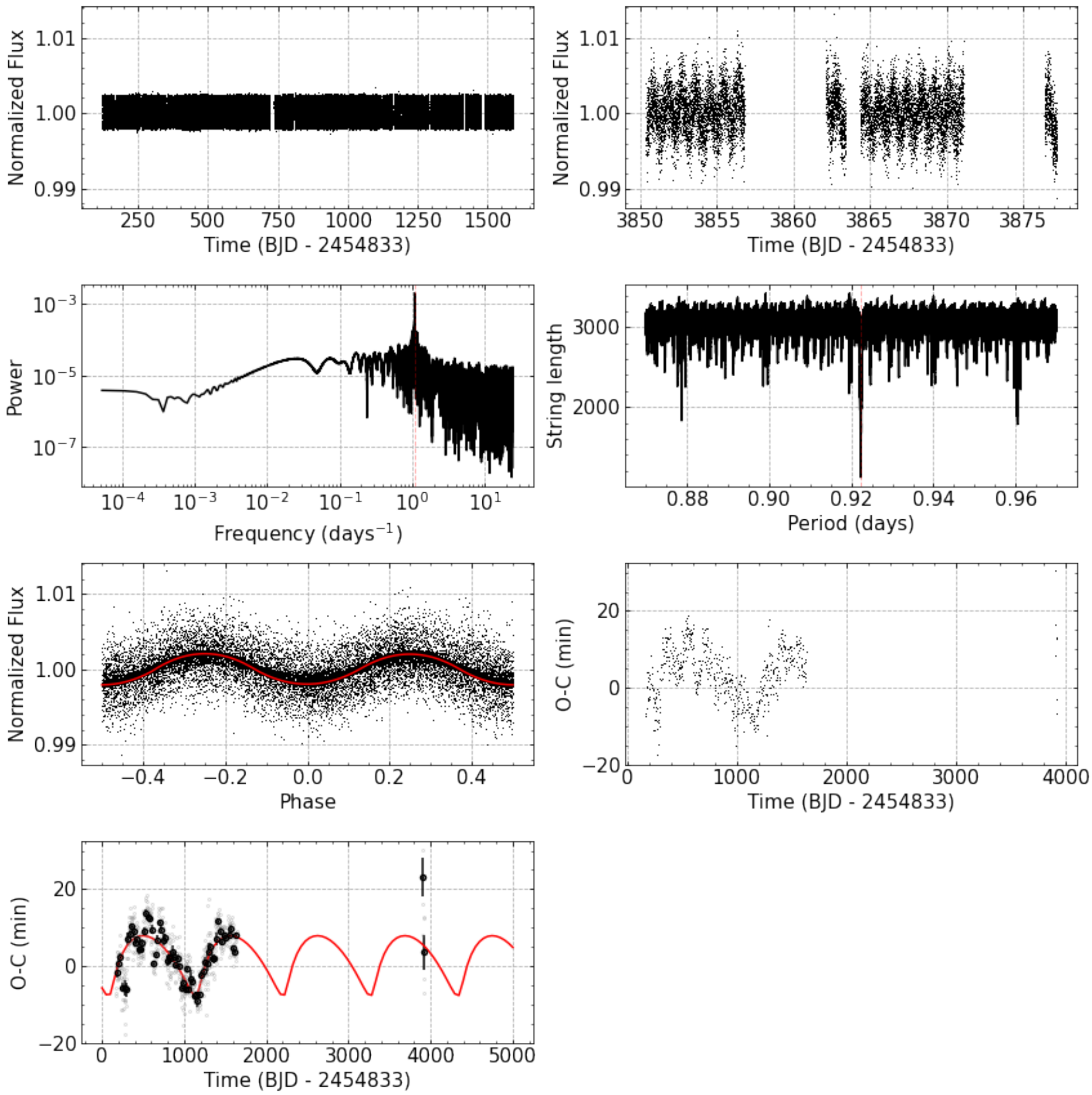

Figure A1. From left to right and top to bottom, respectively: (i) Kepler lightcurve, (ii) TESS lightcurve, (iii) Lomb-Scagle periodogram, (iv) string length periodogram, (v) lightcurve in phase, (vi) O-C diagram, and (vii) O-C diagram with the best fit for the third body candidate.

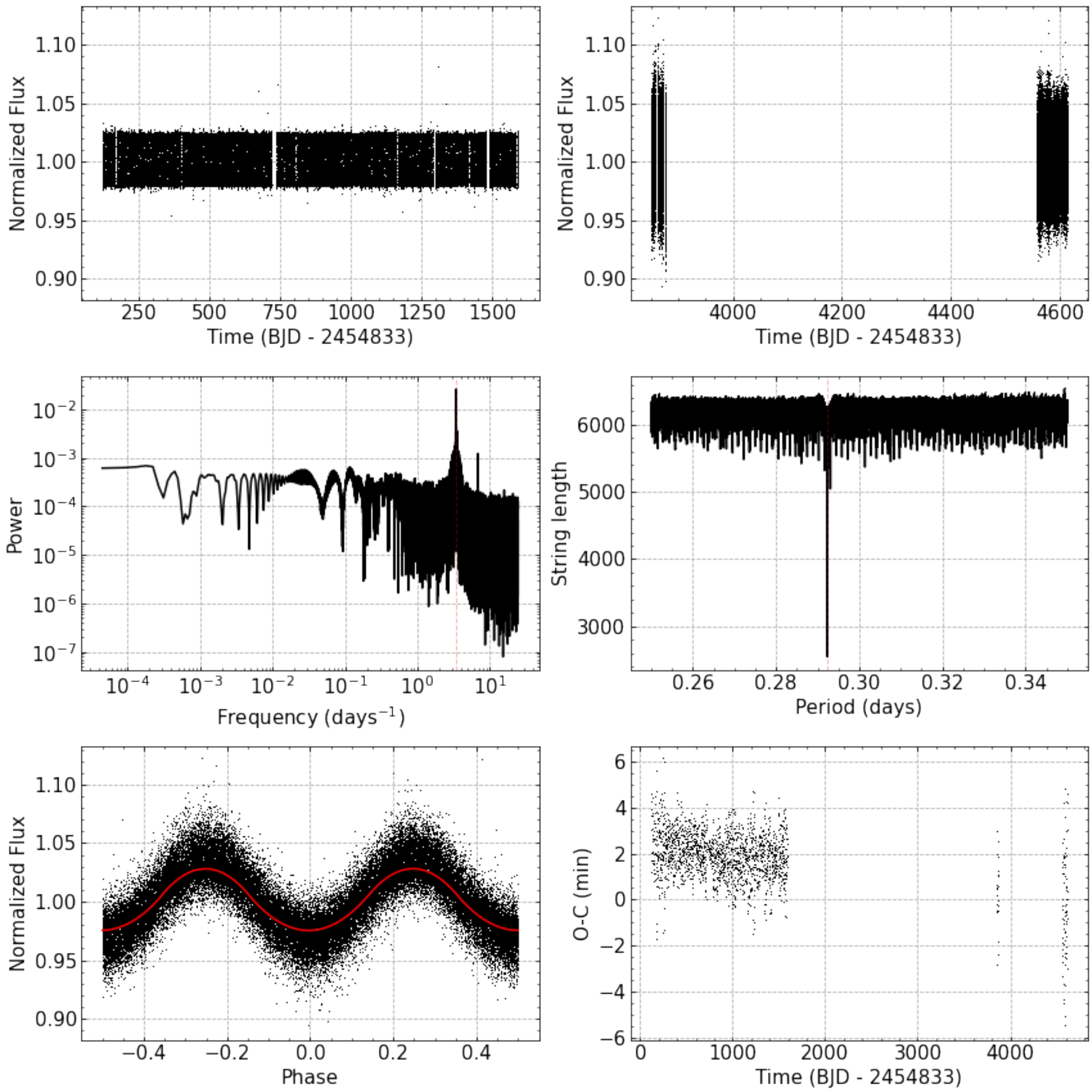

Figure B1. From left to right and top to bottom, respectively: (i) Kepler lightcurve, (ii) TESS lightcurve, (iii) Lomb-Scagle periodogram, (iv) string length periodogram, (v) lightcurve in phase, and (vi) O-C diagram.

Table C1 – *continued* C1.

KIC	P_3 (d)	T_3 (BJD-2454833)	e_3	$a \sin i$ (au)	ω (°)	A (min)	B (min/d)
9832227	6091^{+143}_{-115}	166^{+38}_{-39}	$0.507^{+0.028}_{-0.047}$	$2.824^{+0.023}_{-0.117}$	$313.9^{+1.3}_{-6.0}$		
10155563	3569^{+17}_{-16}	3655^{+22}_{-31}	$0.9890^{+0.0010}_{-0.0020}$	$1.19^{+0.25}_{-0.21}$	$219.0^{+10.3}_{-6.7}$		
10226388	$924.4^{+9.4}_{-1.9}$	291^{+14}_{-23}	$0.518^{+0.238}_{-0.031}$	$0.97^{+0.21}_{-0.12}$	$73.5^{+5.7}_{-11.6}$		
10259530	4584^{+136}_{-316}	4678^{+222}_{-293}	$0.558^{+0.040}_{-0.044}$	$0.258^{+0.010}_{-0.011}$	112^{+23}_{-16}	$2.85^{+0.16}_{-0.12}$	$-0.000800^{+0.000050}_{-0.000060}$
10389982	2300^{+103}_{-37}	4974^{+280}_{-93}	$0.839^{+0.111}_{-0.090}$	$0.1660^{+0.0058}_{-0.0102}$	331^{+21}_{-15}	$5.09^{+0.23}_{-0.22}$	$-0.00130^{+0.00010}_{-0.00010}$
10481912	4102^{+96}_{-510}	4751^{+370}_{-412}	$0.35^{+0.14}_{-0.12}$	$0.378^{+0.030}_{-0.030}$	56^{+36}_{-30}	$4.86^{+0.51}_{-0.34}$	$-0.00160^{+0.00010}_{-0.00020}$
10485137	5844^{+412}_{-145}	$266.8^{+7.9}_{-11.3}$	$0.639^{+0.072}_{-0.064}$	$0.8396^{+0.0848}_{-0.0055}$	$129.1^{+7.0}_{-2.7}$		
10711938	6689^{+261}_{-316}	7381^{+229}_{-552}	$0.631^{+0.250}_{-0.059}$	$0.82^{+0.22}_{-0.14}$	19^{+20}_{-11}		
10724533	1936^{+52}_{-29}	1222^{+481}_{-22}	$0.426^{+0.035}_{-0.185}$	$0.375^{+0.014}_{-0.027}$	$218.297^{+7.6}_{-5.9}$	$7.41^{+0.99}_{-0.23}$	$-0.00220^{+0.00030}_{-0.00010}$
10789421	456^{+10}_{-18}	723^{+23}_{-14}	$0.52^{+0.28}_{-0.18}$	$0.628^{+0.128}_{-0.068}$	$8.9^{+17.9}_{-7.3}$	$9.26^{+0.35}_{-0.45}$	$-0.00950^{+0.00060}_{-0.00030}$
10818544	1872^{+164}_{-114}	1689^{+62}_{-67}	$0.972^{+0.010}_{-0.021}$	$0.802^{+0.087}_{-0.236}$	$357.3^{+2.2}_{-3.9}$	$1.7^{+0.13}_{-0.13}$	$0.000050^{+0.000020}_{-0.000010}$
10979669	1532^{+55}_{-21}	1586^{+91}_{-25}	$0.9740^{+0.0080}_{-0.0130}$	$1.39^{+0.15}_{-0.32}$	$356.0^{+1.4}_{-2.4}$	$-0.0220^{+0.0080}_{-0.0020}$	$0.00030^{+0.00010}_{-0.00020}$
11255667	4715^{+412}_{-203}	421^{+71}_{-59}	$0.27^{+0.11}_{-0.14}$	$0.468^{+0.041}_{-0.027}$	$331.4^{+16.4}_{-9.5}$	$2.90^{+0.34}_{-0.91}$	$-0.00210^{+0.00030}_{-0.00020}$
11572643	2290^{+48}_{-47}	740^{+193}_{-57}	$0.50^{+0.31}_{-0.20}$	$0.784^{+0.039}_{-0.078}$	16^{+39}_{-15}		
12157987	2662^{+58}_{-38}	2371^{+34}_{-46}	$0.914^{+0.034}_{-0.057}$	$0.3471^{+0.0136}_{-0.0087}$	283^{+11}_{-15}	$1.87^{+0.13}_{-0.16}$	$-0.000770^{+0.000030}_{-0.000040}$
12216817	1509^{+28}_{-41}	1244^{+24}_{-39}	$0.619^{+0.071}_{-0.084}$	$0.370^{+0.034}_{-0.029}$	$323.2^{+7.5}_{-10.8}$		
12305537	$2044.343^{+6.0}_{-6.3}$	1850^{+13}_{-19}	$0.707^{+0.037}_{-0.038}$	$1.95^{+0.14}_{-0.16}$	$4.8^{+1.9}_{-2.0}$	$-0.757^{+0.055}_{-0.049}$	$0.000880^{+0.000040}_{-0.000050}$